

pubs.acs.org/JPCC Article

Identification of Stable Perfluorocarbons Formed by Hyperthermal Decomposition of Graphite Fluoride Using Anion Photoelectron Spectroscopy

Published as part of The Journal of Physical Chemistry virtual special issue "Cynthia Friend Festschrift". Brett A. Williams, A. R. Siedle, and Caroline Chick Jarrold*



Cite This: J. Phys. Chem. C 2022, 126, 9965-9978



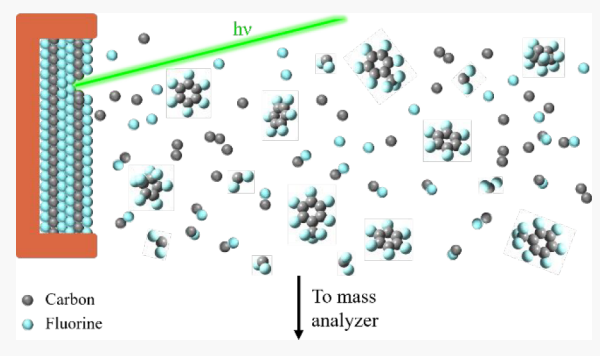
ACCESS I

III Metrics & More

Article Recommendations

Supporting Information

ABSTRACT: Anion photoelectron (PE) spectroscopy was used to characterize several perfluorocarbon (PFC) species generated from pulsed-laser ablation of graphite fluoride (GF) and compare them to PFCs introduced into the gas phase and negatively charged by using a gentle photoemission source. The PE spectra of $C_6F_6^-$, $C_7F_8^-$, and $C_5F_8^-$ produced by ablation of GF are nearly identical with the PE spectra of the anions of hexafluorobenzene, perfluorotoluene, and perfluorocyclopentene, respectively, generated by electron attachment to the neutral perfluorocarbon molecules. This result suggests that laser ablation of GF, which is a hyperthermal decomposition event, produces species larger than CF_2 and with stable molecular structures. In addition, anion PE spectra were obtained for several larger PFC molecular anions, some



of which have been the subject of past computational studies. The electron affinities of these species cannot be determined unambiguously from the broad PE spectra, though a systematic approach to identifying the onset of detachment signal was used to approximate the electron affinities. The vertical detachment energy of perfluoroethylcyclohexene was determined to be 2.98 ± 0.05 eV. The vertical detachment energies of additional perfluorocarbon radical anions, including perfluoroheptene, perfluoromethylcyclohexane, perfluoro-1,3-dimethylcyclohexane, and perfluorodecalin, all exceed 3.495 eV. We also demonstrated that photoemission from gadolinia (Gd₂O₃) using a pulsed laser is an efficient and effective method of generating radical anions of larger volatile molecules in the gas phase.

I. INTRODUCTION

Fluorocarbons (FCs) have become commonplace in many varied industries with numerous applications due to a few key properties. Their high thermal stability, chemical inertness, hydrophobicity, and low viscosity make them ideal for lubricants, 1,2 surfactants, 5 solvents, 6-8 refrigerants, 1,1 and aerosols. 11,12 Cyclic perfluorocarbons (PFCs) are nontoxic and readily dissolve gases such as oxygen and carbon dioxide, so they have shown intriguing promise in the medical field as anesthetics, 13,14 as blood substitutes, 15,16 and for liquid breathing. In addition, they can be detected at extremely low concentrations, making them ideal candidates for chemical tracers. 20–22

This interesting class of molecules has been the subject of theoretical and experimental studies for several decades, with electron binding energies receiving considerable interest. In particular, perfluorinated alkanes and aromatics have been studied extensively by Schaefer and co-workers and were found to have moderate positive electron affinities (EAs), making them ideal e⁻ acceptors.^{23–32} They proposed that perfluorinated polycyclic aromatic hydrocarbons and other large PFCs

could be used to study reactive intermediates related to materials synthesis. They also performed computational studies on linear perfluoropolyacenes. Linear polyacenes, such as pentacene, have been proposed as useful materials for electronics applications, such as transistors and conductors. Perfluoropolyacenes tend to have higher EAs and a lower HOMO–LUMO gap, which could make them more ideal in electronics applications than their unsubstituted counterpart. However, experiments that directly measure the EAs of these species have lagged behind, with only several reports in the literature.

At the bulk limit of PFCs, graphite fluoride (GF) is a material with similar properties to other FCs, such as high lubricity, hydrophobicity, and thermal stability at moderate

Received: March 30, 2022 Revised: May 15, 2022 Published: June 2, 2022





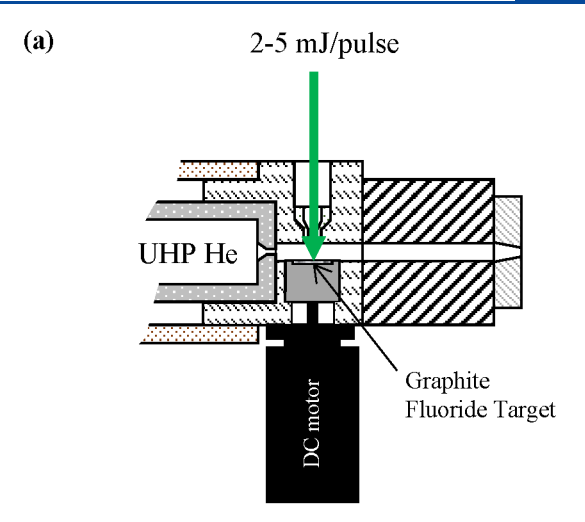
temperatures. GF is used as a lubricant as well as an additive to paint to prevent water damage $^{40-43}$ and has been studied more recently as a cathode material in batteries with encouraging results. However, for GF to be an effective material for widespread use, it needs to be stable and have few unwanted byproducts if it does deteriorate. Thermal decomposition of GF can occur at temperatures as low as 420 $^{\circ}\text{C},^{50-52}$ so it is important to understand the byproducts of this decomposition. 50,53

We recently reported the results of a mass-spectrometrybased study of the products of pulsed-laser ablation and desorption of GF as an attempt to model hyperthermal decomposition. A broad distribution of fluorocarbon species was produced. Many of those species exhibited evidence of further decomposition while undergoing acceleration into the mass spectrometer via loss of CF_2 , forming species having m/zconsistent with the anions of stable, common PFCs. 34 As a complement to that study, we present the photoelectron (PE) spectra of several prominent anions generated by ablation/ desorption of GF, in addition to the anion PE spectra of the anions of stable PFC precursor molecules with the same molecular formulas. The latter are introduced into the gas phase, and an electron is gently attached using a photoemission source to keep their structures intact. These experimental data complement the numerous theoretical studies that have been undertaken to determine the structures and EAs of perfluorocarbons.

II. METHODS

Laser Ablation. Ions were generated, mass selected, and photodetached by using an instrument previously described in detail, 55 though this study introduces a new ion source to complement the source used in previous studies, the latter of which we describe here in brief. Figure 1a shows a schematic of the source used to generate anionic products of GF decomposition by focusing 2-5 mJ/pulse of the second harmonic output of a Nd:YAG laser (532 nm, 2.330 eV), operated at 30 Hz, onto the surface of a compressed GF target, coupled to a pulsed molecular beam valve by a Smalley-type cluster ion source. 56,57 The resulting mixture of fragments is entrained in a pulse of ultrahigh purity (UHP) helium carrier gas (30 psig) through a 2.5 cm long and 0.3 cm diameter channel, where they partially thermalize before expanding into a vacuum. The gas mixture passes through a 3 mm diameter skimmer, whereupon the negatively charged species are accelerated on axis to 1 keV into a time-of-flight (TOF) mass spectrometer. The ions collide with a dual microchannel plate (MCP) detector assembly at the end of the drift tube, and drift times are observed and recorded by a digitizing oscilloscope.

Photoemission Ion Source. To have a point of comparison for the PE spectra of the GF-based anions, we recorded the PE spectra of PFC anions which have the same molecular formulas suggested by the m/z of the GF-based anions. To generate the radical doublet negative ions of the stable commercially available PFCs, we adapted the method of pulsed-laser photoemission pioneered by Schlag et al. with similar approaches subsequently developed by others. Our incarnation, shown in Figure 1b, uses the same source setup described in the previous section, with three modifications. First, instead of situating the target molecule in the cluster source, we inserted a Gd_2O_3 disc, prepared by compressing Gd_2O_3 powder into the sample holder, to serve as a



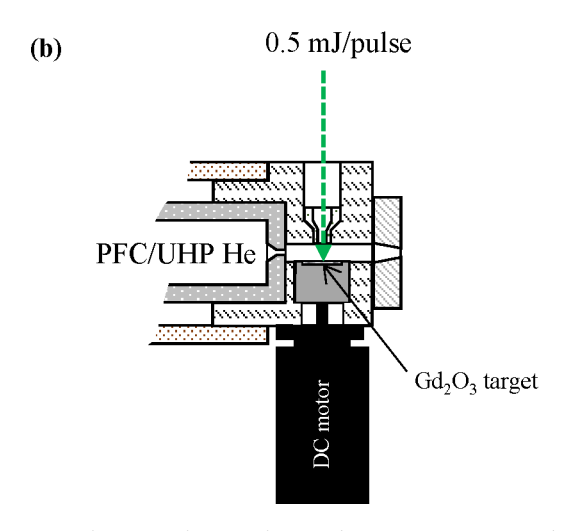


Figure 1. Schematics showing the two distinct ion sources used in this study. (a) $^{GF}C_xF_y^{-}$ ions were generated by direct laser ablation and desorption of a graphite fluoride target using a 2–5 mJ/pulse of the 532 nm output of a Nd:YAG laser, with entrainment in a UHP He pulse. (b) Anions of stable perfluorocarbons were generated by expanding UHP He seeded with the parent molecule into the same source. As the expansion passes over at Gd_2O_3 target, a lower-power laser pulse (ca. 0.5 mJ/pulse) is used to stimulate photoemission of low-energy electrons that attach to the parent molecules.

photoemitter. Second, a reservoir for holding the liquid FC samples was inserted in line with the helium buffer gas, with care taken to thoroughly purge the reservoir when switching PFC samples.

The PFC-seeded He gas is then introduced to the gas phase by a pulsed molecular beam valve, fitted with the source described above. While the PFC-seeded He gas passes over the Gd_2O_3 , less than 1 mJ/pulse of the second harmonic output of a Nd:YAG laser (532 nm, 2.330 eV) operated at 30 Hz impinges on the Gd_2O_3 target, generating electrons. Gd_2O_3 was chosen because the work function has been reported to be lower than 2.330 eV. The laser was operated at powers below the threshold for ablation of the target. The third modification is that the clustering channel was removed to minimize the chance for clustering of the FC anions with neutrals

Table 1 lists the PFCs introduced into the gas phase in this study, along with the m/z value of the resulting anions. Details on the supplier and purities of each sample are included in the

Table 1. List of PFCs Introduced to the Mass Spectrometer Using the Photoemission Ion Source, Including the Molar Mass for Each Molecular Formula and the m/z Value for Any Major Anions Produced

name	formula	$MW (g mol^{-1})$	anion	m/2
hexafluorobenzene	C_6F_6	186.06	$C_6F_6^-$	186
octafluorocyclopentene	C_5F_8	212.04	$C_{5}F_{8}^{-}$	212
octafluorotoluene	C_7F_8	236.06	$C_{7}F_{8}^{-}$	236
			$C_{7}F_{7}^{-}$	217
			unknown	202
perfluoro(methylcyclopentane)	CF_3 - c - C_5F_9	300.05	CF ₃ -c-C ₅ F ₉ ⁻	300
tetradecafluoromethylcyclohexane	CF_3 - c - C_6F_{11}	350.05	CF_3 - c - $C_6F_{11}^-$	350
			$C_{7}F_{8}^{-}$	236
perfluoroheptane			$C_{11}F_{15}^{-}$ (low intensity)	416
			$C_7F_{17}^{-}$	407
			$C_8F_{16}^-$ (low intensity)	400
	C_7F_{16}	388.05	$C_7F_{16}^{-}$	388
			unknown	378
			unknown (low intensity)	366
			$C_7F_{14}^{-}$	350
hexadecafluoroethylcyclohexane	C_2F_5 -c- C_6F_{11}	400.06	$C_8F_{16}^{-}$	400
	(C_8F_{16})		unknown	378
			$C_8F_{14}^-$	362
			$C_7F_{13}^-$	331
			$C_7F_{12}^-$	312
			$C_7F_{11}^-$	293
			$C_6F_{11}^-$	281
			$C_6F_{10}^-$	262
perfluoro(1,3-dimethylcyclohexane)	$1,3-(CF_3)_2-c-C_6F_{10}$	400.06	$1,3-(CF_3)_2-c-C_6F_{10}^-$	400
			$C_7F_{14}^-$	350
octade cafluoro de cahy dron aphthalene	$C_{10}F_{18}$	462.08	$C_{10}F_{18}^{-}$	462
			$C_{10}F_{17}^{-}$	443

Supporting Information (Table S1 and Figures S1–S5). The PFC anions generated from this method will be designated by their molecular formulas (e.g., $C_6F_6^-$) while those generated from laser ablation of graphite fluoride will be distinguished with a superscript GF (e.g., $^{GF}C_6F_6^-$).

Anion PE Spectroscopy. Approximately 20 cm upstream of the ion detector, the ions are selectively photodetached by a pulse of the third harmonic of a Nd:YAG laser (355 nm, 3.495 eV) operated at 30 Hz. The fraction of detached photoelectrons that are ejected perpendicular to the ion beam and laser pulse travel up the 1 m field-free drift tube to be detected by another dual MCP assembly, the signal from which is recorded by a digitizing oscilloscope.

Calibrating with the well-known photoelectron spectra of O⁻ and OH⁻ allows us to convert the electron drift times into electron kinetic energy (e⁻KE). The photoelectron spectra below are plotted as a function of electron binding energy (e⁻BE), which is the energy difference between the final neutral state and the initial state of the anion. It is related to e⁻KE by

$$e^{-}KE = h\nu - EA_0 - E_{int}^{neutral} + E_{int}^{anion} = h\nu - e^{-}BE$$
 (1)

Here, $\mathrm{EA_0}$ is the adiabatic electron affinity of the neutral, $E_{\mathrm{int}}^{\mathrm{neutral}}$ is the internal energy of the neutral (vibrational, rotational, and electronic energy), and $E_{\mathrm{int}}^{\mathrm{anion}}$ is the internal energy of the anion, which is taken to be near zero due to the supersonic expansion, which cools the anions (and neutrals) in the gas mixture plume. The internal energy spread of the final neutral states is governed by the Franck–Condon envelope of vibronic levels accessed in the detachment transition.

The photoelectron spectra were collected by using detachment laser polarization either parallel ($\theta=0\pm10^\circ$) or perpendicular ($\theta=90\pm10^\circ$) to the direction of electron detection. This was done to determine the anisotropy parameter, β , defined as

$$\beta = \frac{I_0 - I_{90}}{0.5I_0 + I_{90}} \tag{2}$$

This value is +2 for photoelectron angular distributions parallel to the laser polarization, -1 for angular distributions perpendicular to the laser polarization, and 0 for isotropic distributions. In the anion PE spectra of large molecular systems such as those presented below, relating β to the symmetry of the orbital associated with the detachment transition is not straightforward. However, variations in β within a congested spectrum can help identify the presence of overlapping electronic transitions.

The energy resolution of the photoelectron energy analyzer is dependent on e⁻KE and is given by

$$\Delta E = 0.004 \text{ eV} + 0.0078 \text{ eV} \left(\frac{e^{-}KE}{eV}\right)^{3/2}$$
 (3)

This is sufficient for resolving vibrational progressions in many cases. As will be described below, no distinct vibrational progressions are discerned in this study. Given the resolution, this observation is consistent with the excess electron structurally distorting the anion relative to the neutral. The spectra shown are collected with between 120000 and 1480000 laser shots at both polarizations (see Table S2 in the Supporting Information). The PE spectra are plotted

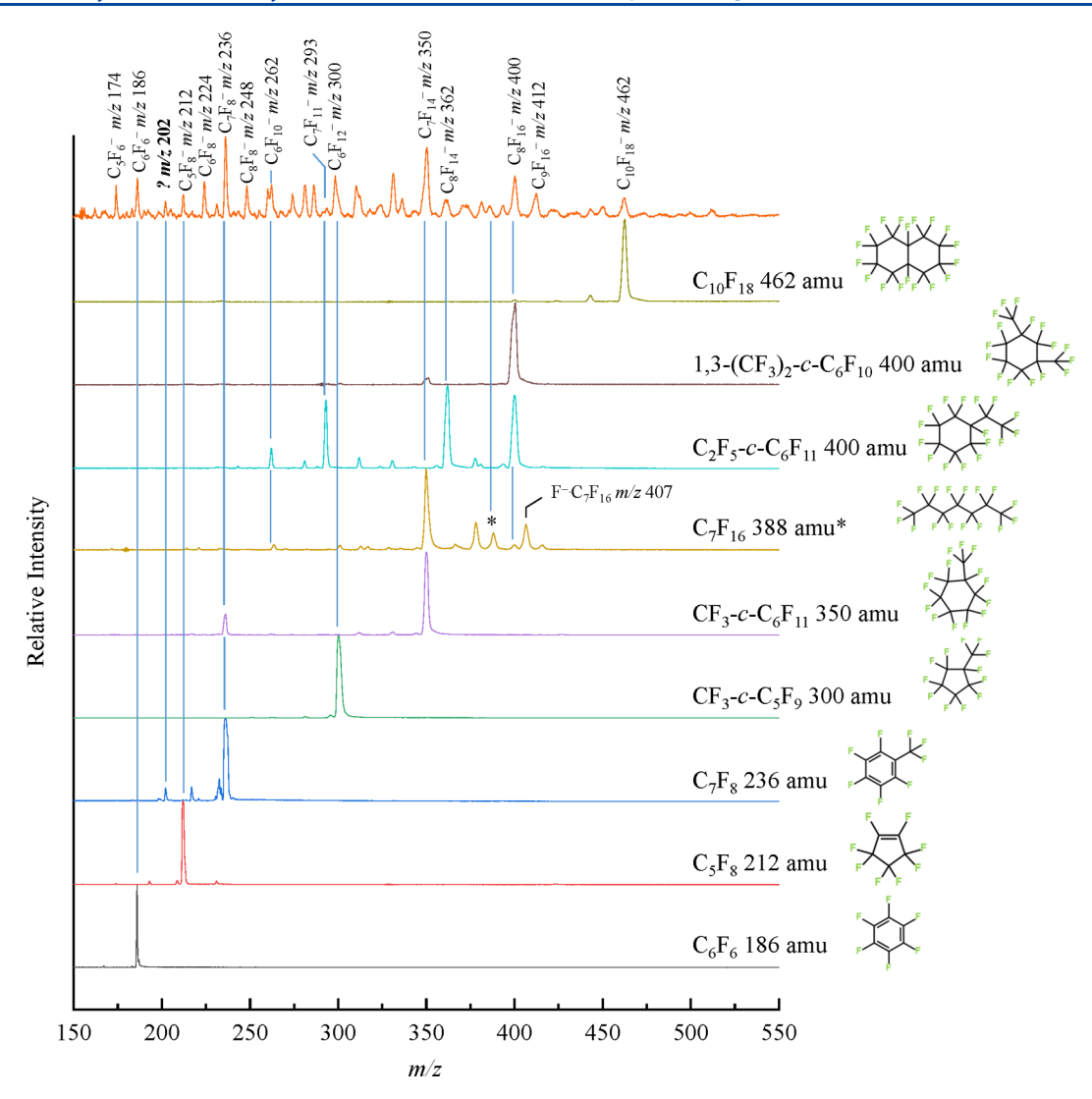


Figure 2. Characteristic mass spectrum of anions generated from laser ablation of GF (top trace) along with the mass spectra of perfluorocarbon species introduced into the gas phase and negatively charged via laser-induced photoemission of electrons. The asterisk (*) indicated m/z consistent with $C_7F_{16}^-$.

against e⁻BE in eV, and the data are binned into equal-energy increments by integrating all the electrons within a given (variable) time interval corresponding to 2 meV.⁶³

Computational Methods. Calculations on the structures of C_xF_v⁻ molecular anions, assuming they are largely preserved relative to the initial neutral reagents used in this study, along with the respective neutral structures, were performed by using the Gaussian 16 suite of computational software to verify positive electron affinities and determine the structural effect of electron attachment.⁶⁴ Structures were optimized by using the Becke, three-parameter, Lee-Yang-Parr (B3LYP) density functional level of theory. Calculations were performed by using the 6-311G basis set supplemented with diffuse functions, three sets of d functions, and one set of f functions (6-311+G(3df)), similar to calculations performed previously on similar species. 65-67 Additionally, B3LYP calculations were completed by using the 3-21G* and 6-31+G basis sets to determine the structures of several species for which calculations did not converge with the larger basis set. These results were used to compute the adiabatic electron affinities, EA₀, which is the difference between the zero-point corrected energies of the optimized structures of the neutral and anionic

molecules. We also calculated the vertical detachment energy (VDE) from the difference in energy between the neutral confined to the structure of the optimized anion and the energy of the anion (not ZPE-corrected).

III. RESULTS

Mass Spectra of PFC Anions versus Ablation of GF.

Figure 2 shows the mass spectra for all molecular $C_x F_y^-$ anions generated by using the photoemission source, along with the mass spectrum of anions generated from ablation of GF, which is consistent with the mass spectrum published previously. The molecular structures for the neutral PFC precursors are shown along with the mass spectra.

While the intent of comparing the mass spectrum of ions generated from ablation of GF with the individual PFCs is not to account for all ions in the former, there are numerous matches between the ions in the PFC mass spectra and the top panel. This includes ions in the PFC mass spectra that cannot be attributed to simple electron attachment to the neutral molecule. A more comprehensive collection of PFCs might have yielded more matches with the GF mass spectrum. However, the GF mass spectrum is also anticipated to be

populated by ions formed from atomization and clustering—a process that is very different from electron attachment and can produce a more diverse ion distribution. The main goal of the current effort is to ascertain whether "magic" ions in the GF mass spectrum have stable PFC molecular structures.

While several of the PFC mass spectra show multiple peaks, most have one primary intense feature with the anticipated m/z, assuming intact molecular anion formation. To account for potential molecular destruction in the photoemission source, we conducted a simple power study. Increasing the power of the laser used to generate the electrons does indeed result in fragmentation and/or atomization of the molecule. As an illustration, Figures 3a,b show mass spectra collected by

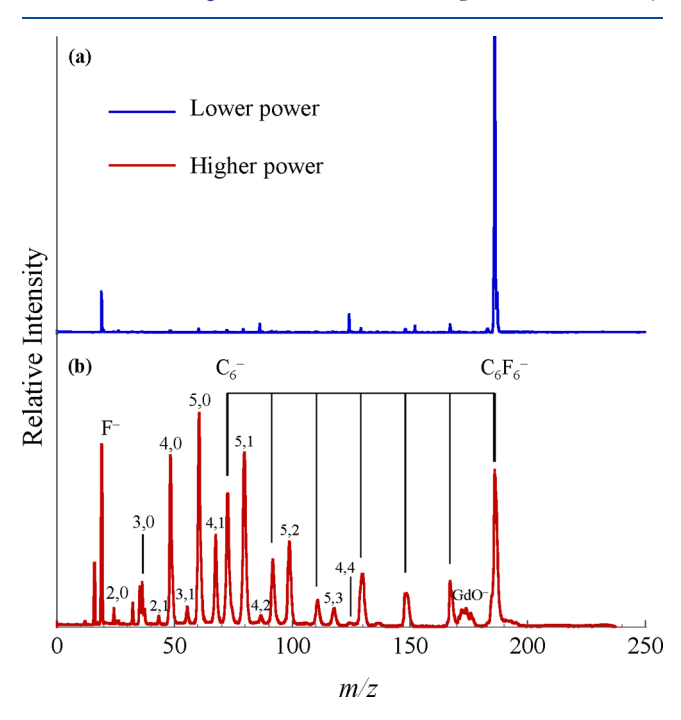


Figure 3. Mass spectra of $C_6F_6^-$ generated using the photoemission source coupled with an expansion of hexafluorobenzene seeded in helium, collected with two different photoemission laser powers. The blue trace (a) was collected by using 1 mJ/pulse, while the red trace (b) was collected by using 2.33 mJ/pulse of the 532 nm (2.33 eV) output of a pulsed Nd:YAG laser.

using C_6F_6 (hexafluorobenzene) as a precursor. Figure 3a shows the mass spectrum collected by using a laser power of 1 mJ/pulse, which exhibits an intense feature assigned to $C_6F_6^-$, and much lower signal associated with F^- and $C_6F_5^-$, which could both form via dissociative attachment, along with several additional lighter ions, including $C_4F_4^-$ and $C_4F_2^-$. Figure 3b shows the mass spectrum collected by using a laser power of 2.33 mJ/pulse. The mass distribution includes C_x^- (x = 2-6), $C_5F_y^-$ (y = 0-3), and $C_6F_y^-$ (y = 0-6) along with the natural isotopic distribution of GdO $^-$. Note that $C_4F_4^-$ and $C_4F_2^-$, both present with low laser power, are *not* more abundant in the distribution of generated with higher power, suggesting they do not form via destruction by the laser.

The mass spectra generated from C_2F_5 -c- C_6F_{11} and C_7F_{16} (n-perfluoroheptane) both show multiple ions. C_7F_{16} is unique in that the ion assigned to $C_7F_{16}^-$, indicated by an asterisk (*) in Figure 2, is low in intensity, while the most intense signal corresponds to the alkene $C_7F_{14}^-$. An ion signal consistent with the $C_7F_{17}^-$ formula, which is more likely to be F^- : C_7F_{16} , is also

observed. Additional species and their m/z values are included in Table 1. n-Perfluoroheptane is predicted to have a positive EA₀, 0.71 eV, by using the B3LYP functional, ²⁶ but the vertical EA is negative. That is, the neutral in its optimized structure does not bind an electron, which might reduce the rate of electron attachment.

The distribution of ions formed from the C_2F_5 -c- C_6F_{11} precursor is similarly more complex than the others (Table 1). Purities were not available for these two compounds, nor for the C_5F_8 sample. Gas chromatographs of these samples indicated that the C_5F_8 sample was pure, while the other samples have multiple components of ambiguous identity (see the Supporting Information). There is therefore no strong evidence that the purported C_2F_5 -c- C_6F_{11} and C_7F_{16} samples are relatively more prone to destruction in the photoemission source. Again, the mass spectra of the remaining cyclic or fluoromethylated cyclic molecules are dominated by a single peak, again with m/z suggesting ion formation by simple electron capture.

PE Spectra of PFC Anions versus GF Ablation Products and Computational Results. The abundance of any given ion generated by ablation of GF is low compared to the very intense ion signal generated by using the photoemission source used to attach electrons to PFCs. As a consequence, direct comparisons between these spectra are limited to ions with m/z consistent with ${}^{GF}C_6F_6^{-1}$, ${}^{GF}C_7F_8^{-1}$, and ${}^{GF}C_5F_8^{-1}$. The PE spectra of the molecular anions generated by using photoemission and ablation of GF are shown in Figures 4-6, with raw PE spectra included in the Supporting Information. All spectra shown here feature broad, congested transitions. Therefore, identification of the EA₀ is difficult due to low or negligible Franck-Condon overlap at the origin and the likely contributions from vibrational hot bands or sequence bands that can appear at e⁻BE values below the EA₀. However, we can systematically identify the e⁻BE value of the onset of electron signal by fitting the rising edge of the band, which serves as our best approximation for the experimental EA₀. These fits are shown in the Supporting Information.

Broad transitions such as those shown below are indicative of significant differences in minimum-energy structures of the anion and associated neutral formed by detachment of the electron. This effect is an indication of the strong antibonding nature of the singly occupied orbital in the doublet anion, as will be explored further in the Discussion section.

 $C_6F_6^-$. We first consider the PE spectra of the hexafluor-obenzene anion ($C_6F_6^-$) and $^{GF}C_6F_6^-$, shown in Figures 4a and 4b, respectively. The PE spectrum of $C_6F_6^-$ was previously reported by Bowen and co-workers, 37 Verlet and co-workers, and Kaya and co-workers. We collected the spectrum on our apparatus for direct comparison; it is nearly identical with the spectrum of Bowen and co-workers in that it exhibits irregularly spaced spikes in signal that hint at very complex partially resolved vibrational combination bands. The spectrum presented by Verlet and co-workers using photoelectron imaging also showed parallel polarization, which is consistent with our spectrum shown in Figure 4a. That is the electrons are ejected preferentially parallel to the electric field of the linearly polarized detachment laser.

The PE spectra of $C_6F_6^-$ (Figure 4a) and $^{GF}C_6F_6^-$ (Figure 4b) are very similar, in terms of both the onset of signal and VDE, as summarized in Table 2, as well as the photoelectron angular distribution, which supports the idea that $C_6F_6^-$ and

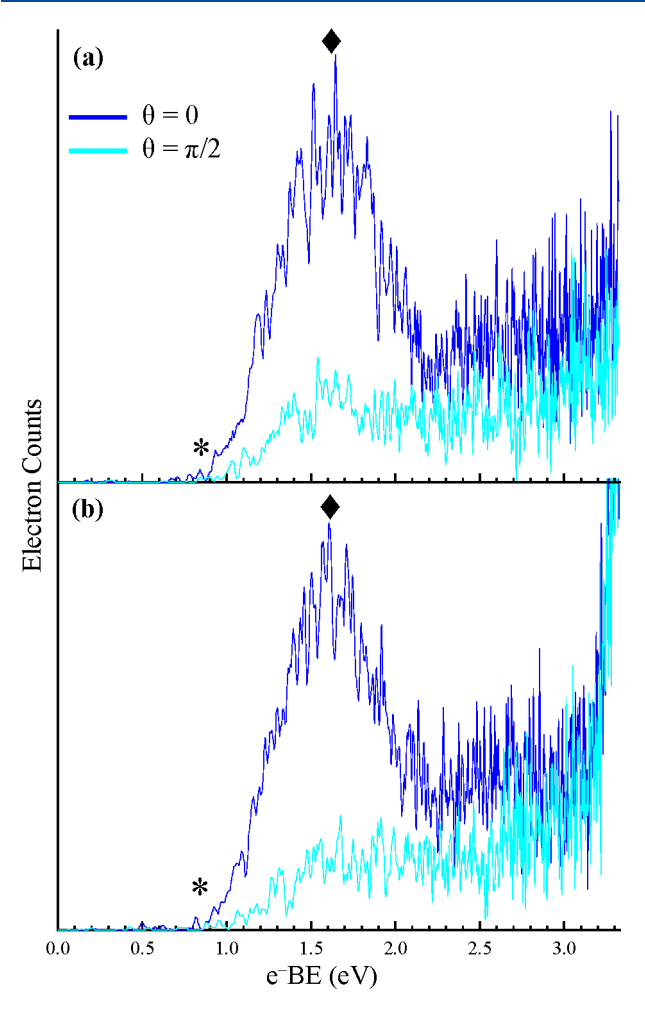


Figure 4. Anion photoelectron spectra of (a) $C_6F_6^-$ generated by flowing neutral perfluorobenzene through the photoemission source and (b) $^{GF}C_6F_6^-$ generated by ablation of GF. The approximate EA₀ is indicated by * and the VDE by ♠. Spectra were collected by using the third harmonic output of a Nd:YAG laser (355 nm, 3.495 eV) with laser polarization parallel (dark blue) and perpendicular (light blue) to the electron drift path.

 $^{\rm GF}{\rm C}_6{\rm F}_6^-$ are structurally the same. Further comparisons of the two sets of PE spectra by polarization and on an expanded scale are shown in Figures S6 and S7. The EA₀ of C₆F₆⁻ is 0.82 \pm 0.05 eV and of $^{\rm GF}{\rm C}_6{\rm F}_6^-$ is 0.82 \pm 0.05 eV, which are in good agreement with the previously reported values of 0.72, 37 0.80, 39 and 0.86 eV. 68 Similarly, the VDEs of C₆F₆⁻ (1.61 \pm 0.05 eV) and $^{\rm GF}{\rm C}_6{\rm F}_6^-$ (1.61 \pm 0.05 eV) are in agreement with the previously reported values of 1.55, 37 1.60, 38 and 1.56 eV. 39

Electron binning conducted on the newly collected spectra presented in Figures 4a,b reveals a platform of continuum signal at e ^-BE values above the main broad transition. Verlet and co-workers noted in their study that the hexafluorobenzene anion has several excited doublet states embedded in the detachment continuum. This continuum signal could therefore represent electronic autodetachment over a wide range of electron kinetic energies due to the coincidental resonance between the detachment laser and high vibrational levels of the D_4 and D_5 excited states of the doublet anion.

Calculations on the hexafluorobenzene anion and neutral using the methods described above compare well with previously reported computational results as well as the experimental spectra. Results of calculations on the optimized

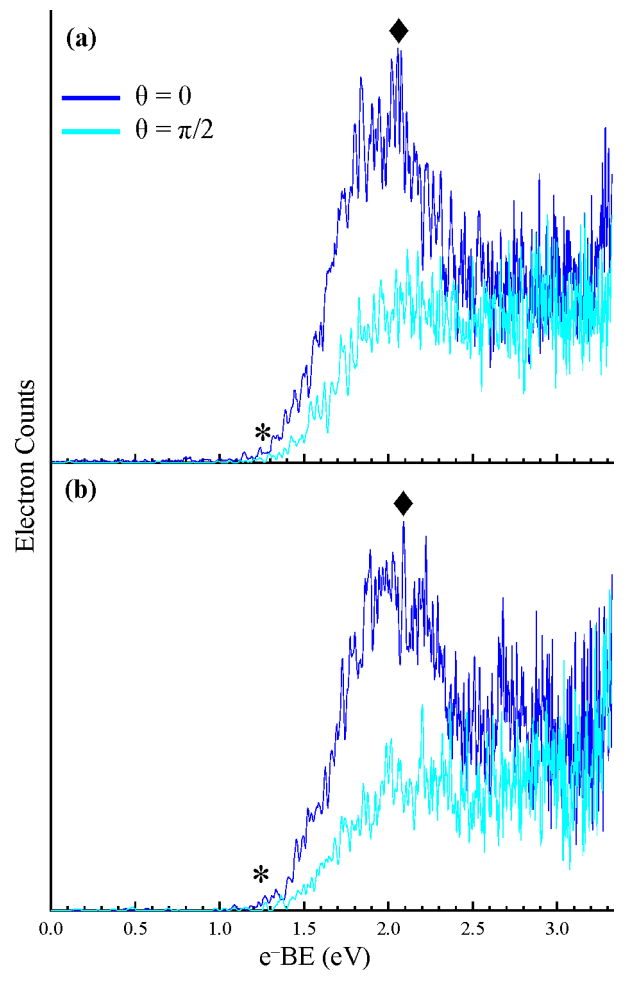


Figure 5. Anion photoelectron spectra of (a) $C_7F_8^-$ generated by flowing neutral perfluorotoluene through the photoemission source and (b) $^{GF}C_7F_8^-$ generated by ablation of GF. The approximate EA₀ is indicated by * and the VDE by ♠. Spectra were collected by using the third harmonic output of a Nd:YAG laser (355 nm, 3.495 eV) with laser polarization parallel (dark blue) and perpendicular (light blue) to the electron drift path.

anion and neutral predict an EA_0 of 0.68 eV, in close agreement with values calculated by Xie et al. (0.69 eV), ²⁴ Hou and Huang (0.72-0.76 eV), ⁶⁷ and Eustis et al. (0.724 eV). ³⁷ Our calculated VDE of 1.59 eV is also in agreement with the value reported by Kaya and co-workers. ³⁹ This agreement is taken as a measure of validation of this computational method in its applications to the other molecules in this study. The experimental and computed detachment energies from this study are summarized in Table 2.

 $C_7F_8^-$. While not the next in order in terms of m/z, the perfluorotoluene neutral and anion (C_7F_8 , $C_7F_8^-$), of all the species studied here, are the most similar to hexafluorobenzene neutral and anion in terms of electronic structure. We therefore present the PE spectra of $C_7F_8^-$ and $^{GF}C_7F_8^-$ in Figures 5a and 5b, respectively. Again, the profiles for the two species are similar, as are the photoelectron angular distributions. That is the main, broad transition in both spectra have parallel distributions, while the continuum plateau of signal to higher e⁻BE is isotropic. The EA₀ of $C_7F_8^-$ is 1.25 \pm 0.05 eV and of $^{GF}C_7F_8^-$ is 1.25 \pm 0.05 eV, which are different from the wide range of values previously reported. Kebarle and co-workers measured the gas-phase electron-transfer equilibria to

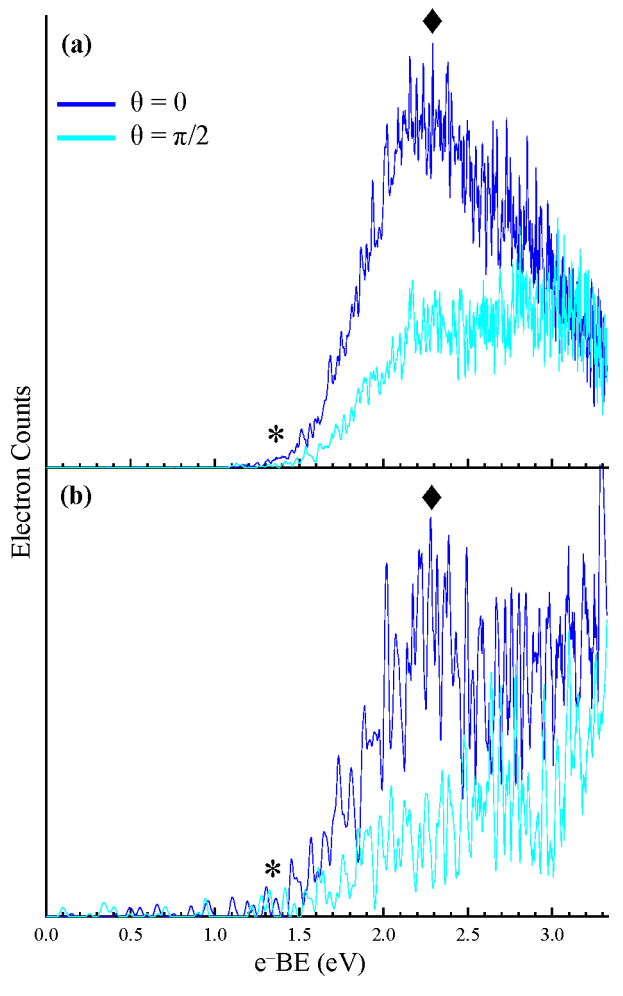


Figure 6. Anion photoelectron spectra of (a) C₅F₈⁻ generated by flowing neutral perfluorocyclopentene through the photoemission source and (b) GFC5F8- generated by ablation of GF. The approximate EA₀ is indicated by * and the VDE by \blacklozenge . Spectra were collected by using the third harmonic output of a Nd:YAG laser (355 nm, 3.495 eV) with laser polarization parallel (dark blue) and perpendicular (light blue) to the electron drift path.

Table 2. Experimental and Computed EA₀ and VDE Values for the Perfluorocarbons Targeted in This Study^a

molecule	exptl EA ₀ /VDE (eV)	calcd EA ₀ /VDE (eV)
hexafluorobenzene	0.82(5)/1.61(5)	0.68/1.59
$^{GF}C_6F_6$	0.82(5)/1.61(5)	
octafluorocyclopentene	1.33(10)/2.30(5)	1.05/2.39
$^{GF}C_5F_8$	1.33(10)/2.3(1)	
octafluorotoluene	1.25(5)/2.06(5)	1.03/2.01
$^{\mathrm{GF}}\mathrm{C}_{7}\mathrm{F}_{8}$	1.25(5)/2.09(5)	
C_8F_{14}	1.55(10)/2.98(5)	
C_7F_{14}	2.25(10)/-	
CF_3 - c - C_6F_{11}	2.20(10)/-	
$1,3-(CF_3)_2-c-C_6F_{10}$	2.38(10)/-	
$C_{10}F_{18}$	2.58(10)/-	

^aVDE values for the species listed toward the bottom of the table are above 3.3 eV. Uncertainty in the last digit(s) is given in parentheses.

determine values for EA₀ of 0.92 eV⁶⁹ and 0.94 eV,⁷⁰ while Lifshitz et al. measured the translational energy thresholds of electron-transfer reactions to determine an EA₀ of 1.7 eV.

The VDE of $C_7F_8^-$ is 2.06 \pm 0.05 eV and of $^{GF}C_7F_8^-$ is 2.09 \pm 0.05 eV.

The calculated EA₀ and VDE values are 1.03 and 2.01 eV, respectively. These values are in good agreement with the experimental values, and our computed EA₀ value is in reasonable agreement with Kebarle and co-workers. 69,70 This result again suggests that the Franck-Condon overlap at the origin is small, resulting in near-zero detachment signal at the associated e⁻BE. The experimental and computed detachment energies from this current work are included in Table 2.

C₅F₈-. The PE spectra of the perfluorocyclopentene anion $(C_5F_8^-)$ and ${}^{GF}C_5F_8^-$ are shown in Figures 6a and 6b, respectively. C_5F_8 has been studied by electron transmission and photoionization previously, and it is known to bind an electron. ^{72–74} The PE spectrum of ^{GF}C₅F₈⁻ presented here has much lower signal-to-noise due to its relatively low abundance in the mass spectrum of the GF ablation products. Therefore, the PE spectrum of GFC5F8 was smoothed to compare its approximate EA₀ and VDE with C₅F₈⁻. The raw PE spectrum is included in the Supporting Information.

The PE spectra of both $C_5F_8^-$ and ${}^{GF}C_5F_8^-$ have the characteristically broad, main transition with matching EA0 and VDE values, within the uncertainty of our measurements. They are higher than the EA₀ and VDE values determined for the aromatic species: the EA₀ is 1.33 eV, and the VDE is 2.3 eV (Table 2). While it is more difficult to compare the photoelectron angular distributions given the low signal-tonoise of the ${}^{GF}C_5F_8^-$ spectrum, they are both parallel, with continuum signal at higher e BE being isotropic. The EA₀ value is in good agreement with the previously calculated values of 1.27 $\,\mathrm{eV}^{65}$ and 1.20 $\,\mathrm{eV}^{.66}$

Our calculated detachment energies again are in good agreement with our experimental values. The EA₀ was calculated to be 1.05 eV, and the computed VDE is 2.39 eV. Both values are in reasonable agreement with the experimental values, 1.33 and 2.3 eV, respectively. Our experimental and computed detachment energies are included in Table 2.

PE Spectra of Larger PFCs. Attempts to measure the PE spectra for several of the larger magic ${}^{GF}C_xF_y^-$ species were unsuccessful due to low ion abundances combined with high electron affinities. However, we did measure the PE spectra for several larger $C_x F_y^-$ anions, including two with an m/z that suggests loss of F₂ from the parent neutral (note, however, that the samples were lower purity, vide supra and the Supporting Information).

 $C_8F_{16}^-$ (m/z 400) is prominent in the mass spectrum of GF (top trace, Figure 2), and ions with the same m/z were produced from negatively charging both 1,3-(CF₃)₂-c-C₆F₁₀ and C₂F₅-c-C₆F₁₁. Despite the high abundances of the anions generated by electron attachment to the two PFCs, we were unable to detach electrons from their respective 400 m/zanions, suggesting that their EA₀, or the lowest e⁻BE at which the detachment cross section is non-negligible, is over 3.3 eV. However, the PE spectrum of the C₈F₁₄ ion observed in the mass spectrum of the C₂F₅-c-C₆F₁₁ sample was measurable with 3.495 eV photon energy, as shown in Figure 7. The EA₀ of this isomer of $C_8F_{14}^-$ is 1.55 \pm 0.05 eV, and the VDE is 2.98 \pm 0.05 eV. The electron binding energy is higher than but comparable to C₅F₈. We therefore propose a structural assignment of perfluoroethylcyclohexene, with fewer F atoms on the central ring, lowering the electron affinity relative to a structure with an F-saturated ring and a perfluorovinyl group. The photoelectron angular distribution is more isotropic than

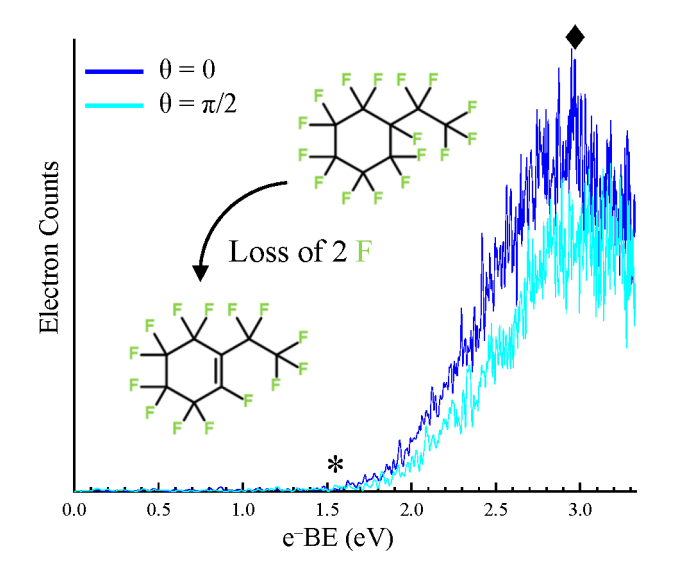


Figure 7. Anion photoelectron spectrum of $C_8F_{14}^-$ generated by flowing neutral C_8F_{16} through the photoemission source. Note that the GC of this sample showed multiple species present in the sample, so loss of F_2 is not necessarily occurring in the ion source. The approximate EA_0 is indicated by * and the VDE by \spadesuit . The spectrum was collected by using the third harmonic output of a Nd:YAG laser (355 nm, 3.495 eV) with laser polarization parallel (dark blue) and perpendicular (light blue) to the electron drift path.

the three species shown in the last subsection. The difference can be attributed to the lower e⁻KE values and the attending higher contribution from s-wave detachment.^{75–77} The raw PE spectrum is shown in the Supporting Information.

Figure 8 shows the PE spectra of the other PFCs for which electron collection was possible with 3.495 eV photon energy. Little information beyond the onset of electron signal, which is an upper limit on the EA₀, can be gleaned from the spectra. The VDE values cannot be determined from these spectra, as it is higher than the 3.3 eV cutoff of our ability to detect electrons in all four cases. They include (a) $C_7F_{14}^-$ from the C_7F_{16} sample, (b) the m/z-coincident CF_3 -c- $C_6F_{11}^-$, (c) 1,3- $(CF_3)_2$ -c- $C_6F_{10}^-$, and (d) $C_{10}F_{18}^-$. Because the photoelectron angular distributions are nearly isotropic for these species, again, because of the low e⁻KEs, electrons collected both parallel and perpendicular to the laser polarization were added in the PE spectra shown to provide better signal-to-noise. The angle-resolved spectra are included in the Supporting Information (Figures S17–S20).

We approximate the EA $_0$ for these species to be 2.25 \pm 0.10 eV (C $_7$ F $_{14}^-$), 2.20 \pm 0.10 eV (CF $_3$ -c-C $_6$ F $_{11}^-$), 2.38 \pm 0.10 eV (1,3-(CF $_3$) $_2$ -c-C $_6$ F $_{10}^-$), and 2.58 \pm 0.10 eV (C $_{10}$ F $_{18}^-$). The values for 1,3-(CF $_3$) $_2$ -c-C $_6$ F $_{10}^-$ and C $_{10}$ F $_{18}^-$ are consistent with previously calculated values by Kim and co-workers, ⁷⁸ and the value for CF $_3$ -c-C $_6$ F $_{11}^-$ is consistent with the photodetachment value measured by Mock and Grimsrud (3.3 eV)⁷⁹ and

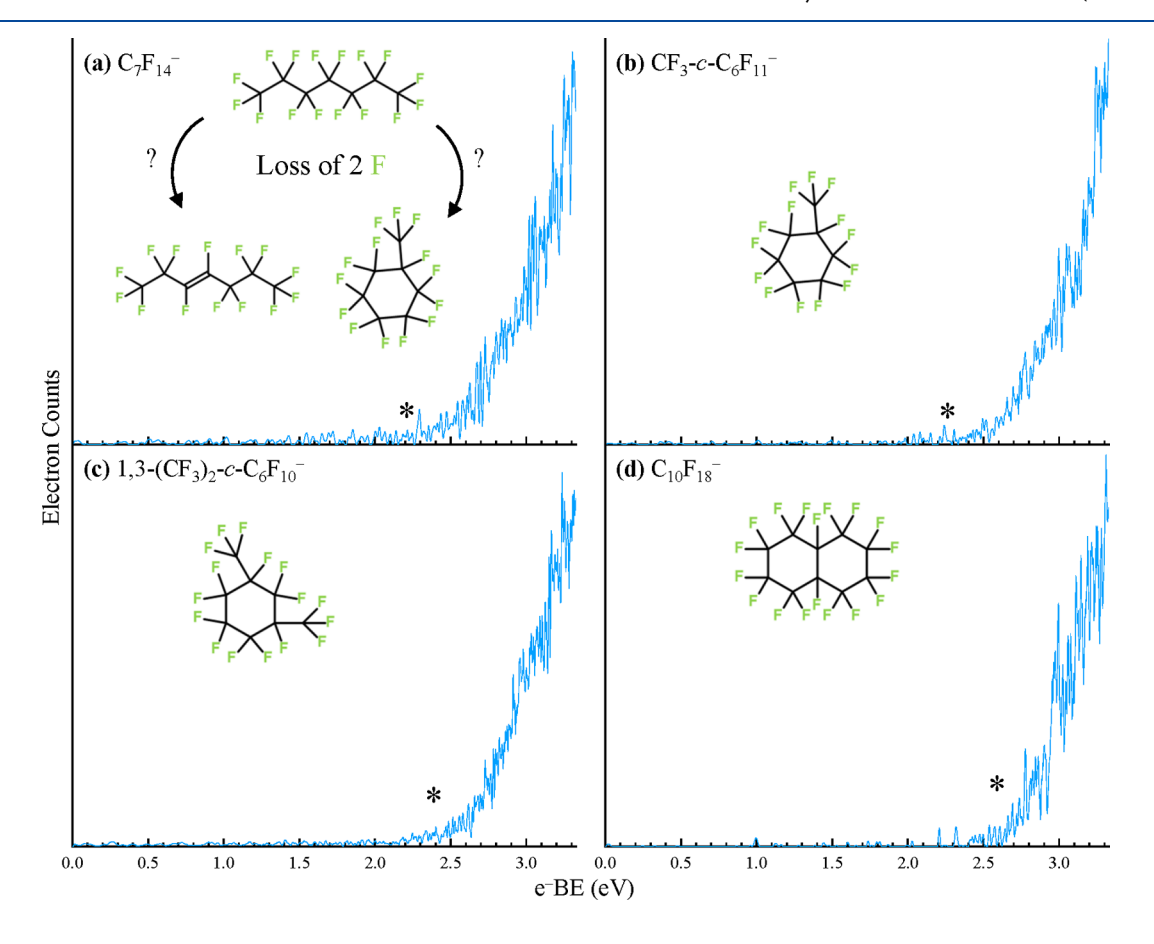


Figure 8. Sum of the anion photoelectron spectra obtained with parallel and perpendicular laser polarizations for (a) $C_7F_{14}^-$ (GC-MS indicated multiple compounds in the sample; loss of F_2 is not necessarily occurring in the ion source), (b) CF_3 -c- $C_6F_{11}^-$, (c) 1,3- $(CF_3)_2$ -c- $C_6F_{10}^-$, and (d) $C_{10}F_{18}^-$ from ionization of neutral PFCs in the gas phase. The approximate EA_0 values are indicated by an asterisk. The structures of the parent neutral precursors are shown in each frame. Spectra were collected by using the third harmonic output of a Nd:YAG laser (355 nm, 3.495 eV).

calculated by Chen and co-workers (3.0 eV).⁸⁰ Our EA₀ values determined from these spectra are included in Table 2.

Close inspection of the PE spectrum of the $C_7F_{14}^-$ anion formed from the n- C_7F_{16} precursor (Figure 8a) and the spectrum of the m/z-coincident CF_3 -c- $C_6F_{11}^-$ anion (Figure 8b) reveals nearly identical profiles. The spectra are shown overlaid in the Supporting Information (Figure S22). The similarity of the spectra raises the question of whether F_2 loss from perfluoro-n-heptane leads to a cyclization of the molecule, forming CF_3 -c- $C_6F_{11}^-$. We attempted calculations on the neutral and anionic isomers of n-perfluoroheptene and CF_3 -c- C_6F_{11} to determine whether they are expected to have similar detachment energies. While we were only able to get calculations with smaller basis sets to converge, the EA $_0$ and VDE values computed for perfluoro-2-heptene and perfluoro-3-heptene are both close to the detachment energies calculated for CF_3 -c- C_6F_{11} . The results are summarized in Table 3. We

Table 3. Computed EA₀ and VDE Values for Three Isomers of n-Perfluoroheptene and CF₃-c-C₆F₁₁ Calculated with B3LYP Density Functional Theory Using the Basis Sets 3-21G*, 6-31+G, and 6-311+G(3df)

	EA_0/VDE (eV)		
molecule	3-21G*	6-31+G	6-311+G(3df)
PF-1-heptene	0.0239/1.67	1.96/3.70	0.711/2.24
PF-2-heptene	0.642/2.04	2.55/3.91	1.25/2.76
PF-3-heptene	0.708/1.60	2.66/3.88	1.32/2.66
CF_3 - c - C_6F_{11}	0.508/3.07	2.99/5.28	

note here that calculations done with different basis sets yield significantly different EA $_0$ and VDE values, but the similarity between the detachment energies of the linear and cyclic isomers is consistent. We therefore do not assert that F $_2$ loss from $n\text{-}\mathrm{C}_7\mathrm{F}_{16}$ results in CF $_3\text{-}c\text{-}\mathrm{C}_6\mathrm{F}_{11}$ formation, but neither can we eliminate the possibility that it is occurring.

EA₀ tends to increase with molecule size from C₇F₁₄ $(350 \ m/z)$ to $C_{10}F_{18}^ (462 \ m/z)$, which has been calculated previously in different perfluoroalkanes^{26,28} and for cyclic PFC radical anions,²⁵ though the fused-ring $C_{10}F_{18}$ structure is clearly different from a simple ring. The trend is not linear with fully saturated single ring size. Other effects, such as perfluoromethyl or perfluoroethyl group substitution on the ring, can significantly increase the EA₀. The previous computational studies reported a trend of EA increasing with PFC size up to five-carbon rings and then decreasing with increasing size. 25,28 However, our results are more similar to the results of Kim and co-workers, who calculated the EA₀ values of C₈F₁₆, C₉F₁₈, and C₁₀F₁₈, predicting a more modest increase in EA₀ with molecule size. ⁷⁸ CF₃-c-C₆F₁₁ was previously reported to have a much lower EA₀. Viggiano and co-workers compared the electron attachment and detachment rate constants of CF₃-c-C₆F₁₁ to get an EA₀ of 1.02 eV and calculated it to be 1.43 eV, 66 while Kebarle and co-workers reported EA₀ to be 1.06 eV from electron-transfer equilibria data.81

Calculations on all of these species are beyond the scope of this paper. However, there are several previous computational studies upon which we can draw. 25,26,28,31,66,78 Schaefer and

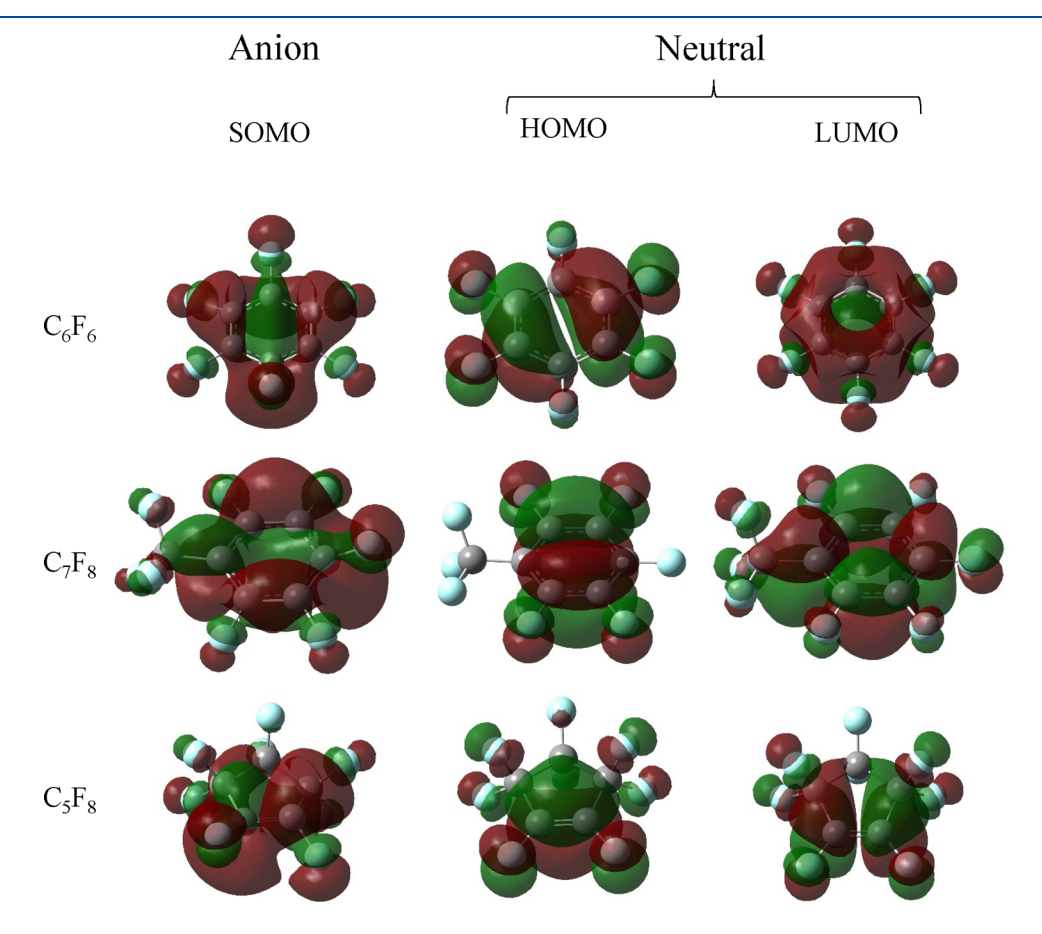


Figure 9. Frontier molecular orbitals of C_6F_6 , C_7F_8 , and C_5F_8 for the optimized anion and neutral structures. Shown are the SOMOs of the anions (left) and the HOMOs (middle) and LUMOs (right) of the neutral species.

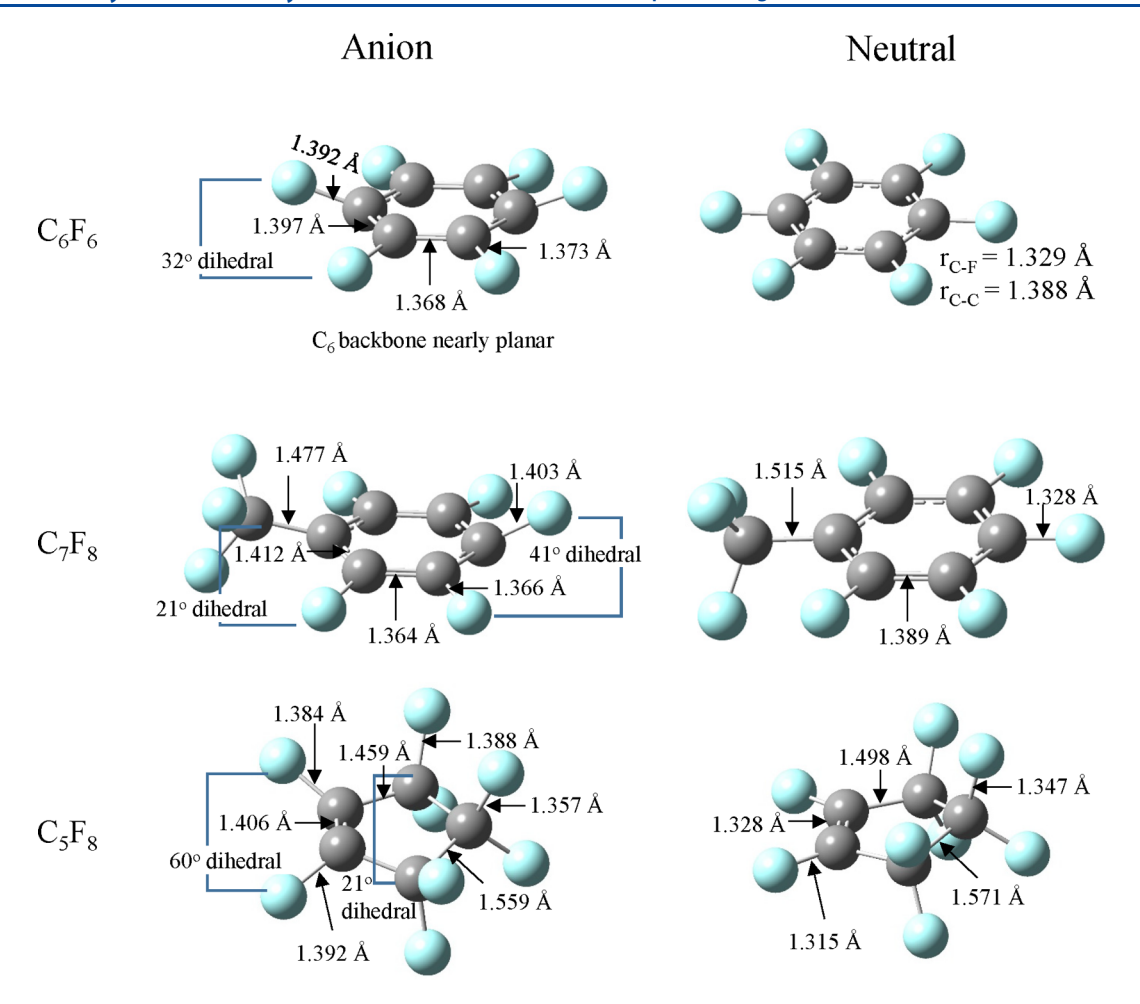


Figure 10. Representative computed structural parameters for the optimized C_6F_6 , C_7F_8 , and C_5F_8 anion and neutral structures.

co-workers calculated the EA_0s and VDEs on a series of saturated cyclic perfluorocarbons, predicting an EA_0 of 1.56 eV for CF_3 -c- C_6F_{11} , which is significantly lower than our observed one of 2.20 eV. However, as noted previously, significant differences between the structures of the neutrals and anions can result in near-zero Franck—Condon overlap between the lowest vibrational levels of the anion and those of the neutral, i.e., near-zero signal intensity near the transition origin, which defines the true EA_0 .

IV. DISCUSSION

Formation of Stable Species from Ablation of GF. As we have previously reported, 54 the mass distribution of anions generated by ablation of GF, which induces hyperthermal decomposition of GF, shows a series of ions that suggest that stable species might form via two different pathways: coalescence of smaller species, such as C and F atoms as well as small CF molecules, or decomposition of larger, desorbed species. As an example, the $C_x F_8^-$ (5 $\leq x \leq 9$) progression of ions, some of which are indicated along the top trace in Figure 2, may suggest sequential C addition to a nucleating species due to collisions in the ion source. The fact that both ${}^{GF}C_5F_8^-$ and ${}^{GF}C_7F_8^-$, the latter being one of the most abundant, or magic, have PE spectra that are nearly identical with the perfluorocyclopentene and perfluorotoluene anions is therefore somewhat surprising. Sequential atom addition to a fragment is a highly exothermic process, so these species would necessarily have ca. 4 eV or more of internal

energy during formation. The similarities in the ${}^{GF}C_xF_y^-$ and $C_xF_y^-$ PE spectra therefore suggest that the residence time in the ion source, which is on the order of tens of microseconds, is sufficient to facilitate annealing and cooling.

Electronic and Molecular Structures of $C_6F_6^-$, $C_7F_8^-$, and $C_5F_8^-$. The caveat to the assertion above—stable perfluorocarbons forming from ablation of GF—is the similarity between all the anion PE spectra shown in Figures 4–6. The EA₀ and VDEs gleaned from the spectra of the distinct molecules are unambiguously distinguishable. However, we cannot unambiguously claim that the EA₀s and VDEs of constitutional isomers of, for example, $C_6F_6^-$ are different from hexafluorobenzene. Nonetheless, the similarity of broad, vibrationally congested photodetachment transitions observed in all the spectra presented here is worth further comment.

Figure 9 shows the frontier orbitals for the anionic and neutral structures of C_6F_6 , C_7F_8 , and C_5F_8 . They include the SOMO (singularly occupied molecular orbital) of each anion, the neutral HOMO (highest occupied molecular orbital), and the neutral LUMO (lowest unoccupied molecular orbital), which correlates to the SOMO of the anion. What is immediately obvious is the striking difference in the appearance of the SOMO of the anion and the neutral LUMO. Stabilization of the excess charge in the anions is achieved by distortion of the molecular structure to minimize the antibonding character of the SOMO. Detachment of the excess electron results in a neutral that is structurally and electronically very different from the minimum-energy neutral

structure. That is significant orbital relaxation along with molecular structural relaxation is expected to occur with photodetachment.

To consider the structural differences in more detail, Figure 10 shows the optimized molecular structures of the C_6F_{6} , C_7F_{8} , and C_5F_8 anions and neutrals. Relative to neutral C_6F_6 , the anion is distorted from the planar D_{6h} to $C_{2\nu}$ symmetry in which two C–F groups para to each other bend above the plane of the ring while the other four C–F groups bend below the plane. C–F bond lengths are longer in the anion because the SOMO has C–F antibonding character (in contrast to the π_3 orbital of benzene). The two equivalent C–C bonds in the anion are predicted to be 0.02 Å shorter than the neutral C–C bonds, while the four equivalent C–C bonds are \sim 0.01 Å longer.

Similarly, $C_7F_8^-$ is distorted from C_s to C_1 symmetry. The CF₃ group and the C-F *para* to it bend above the plane of the C₆ ring while the four remaining C-F groups bend below the plane. Differences in the anion and neutral C-F and C-C bonds are analogous to those predicted for C_6F_6 . The C-CF₃ bond length decreases in the anion because of an increase in C-C bonding character in the SOMO relative to the LUMO of the neutral.

While the C_6 rings in both $C_6F_6^-$ and $C_7F_8^-$ are moderately bent from planar, $C_5F_8^-$ is significantly distorted from C_s to C_1 symmetry with a ring twist which displaces the two CF_2 groups adjacent to C=C above and below the plane of the C=C bond, i.e., the C-C=C-C dihedral angle is 0° (planar) in the neutral, 21° in the anion. The F-C=C-F dihedral angle is 0° in the neutral and 60° in the anion as the two C-F bonds twist above and below the plane of the C=C bond. The C=C bond length increases in the anion due to increased antibonding interactions while the other four C-C bond lengths decrease. All of the C-F bond lengths increase in the anion due to the C-F antibonding character in the SOMO.

The anion and neutral structures of these three species are shown in the side-view of Figure S23.

In sum, for all three, the structures of the anions minimize the antibonding nature of the SOMO, which accounts for the relatively robust EA_0 s of the associated closed-shell neutral molecules.

Beyond these unsaturated species, the EA₀ values are evidently much higher for saturated species. In the unsaturated species C_6F_6 , C_7F_8 , and C_5F_8 , the π -bonds delocalize the excess electron density in the anion. However, in C₆F₆ and C₇F₈, the loss of aromaticity results in relatively low stabilization of the anion relative to the neutral. In contrast, in the more saturated species, the C-centers are more electron deficient than in the unsaturated species. While the excess charge is localized in a C-F σ^* orbital, Schaefer and co-workers found that in branched PFCs, tertiary C-F σ^* orbitals are further stabilized by the adjacent -CF₃ group through negative hyperconjugation. The higher EA₀ values in the large, saturated PFCs are due to the increase in electron-withdrawing groups such as -CF₂ and -CF₃. These were shown by Paul et al. to increase the EA₀ values of the perfluoroalkanes due to the excess electron being in the C-F σ^* orbital at the tertiary carbon, which elongates the C-F bond and isolates the electron density near the highly electronegative F atom. 26,28,31 The trend of increasing EA₀ with increasing size is shown in the Supporting Information.

While a direct comparison between the PE spectra of ${}^{GF}C_xF_y^-$ and $C_xF_y^-$ was limited to $C_6F_6^-$, $C_7F_8^-$, and $C_5F_8^-$, for

these three species that are abundant in the GF ablation mass spectrum the EA_0 and VDE values for each set of species are nearly identical, raising the possibility that the same could be true for the other "magic" ions in the GF mass spectrum. This finding minimally suggests that the hyperthermal decomposition of GF leads to the formation of stable PFCs, which provides further insight into the nature of GF decomposition.

V. CONCLUSIONS

Hyperthermal decomposition of GF via laser ablation studied previously by mass spectrometry exhibited evidence of particularly abundant, or "magic", decomposition products with m/z consistent with stable PFC molecular anions. To complement the study, we utilized a new photoemission source to introduce intact PFCs into the gas phase and measure their PE spectra. These PE spectra were compared to the PE spectra collected for mass-coincident anions generated by laser ablation of GF. The three species generated by ablation of GF for which we were able to collect spectra, GFC₆F₆, ${}^{\mathrm{GF}}\mathrm{C_{7}F_{8}}^{-}$, and ${}^{\mathrm{GF}}\mathrm{C_{5}F_{8}}^{-}$, exhibited PE spectra that were very similar to the PE spectra of the intact hexafluorobenzene, perfluorotoluene, and perfluorocyclopentene anions, respectively. While the spectra of all six of these samples were broad and lacked cleanly resolved vibrational structure, they had sufficiently unique EA₀ and VDE values from which we could infer that the species generated by ablation were predominantly the stable perfluorocarbons. The measured EA₀/VDE values are $0.82 \pm 0.05 \text{ eV} / 1.61 \pm 0.05 \text{ eV}$ for $C_6 F_6^-$, $1.25 \pm$ $0.05 \text{ eV}/2.06 \pm 0.05 \text{ eV}$ for $C_7 F_8^-$, and $1.33 \pm 0.10 \text{ eV}/2.30 \pm$ $0.05 \text{ eV for } C_5 F_8^-$.

We further measured the PE spectra of several larger perfluorocarbon anions introduced into the gas phase using the photoemission source. These larger species have significantly higher EAs, which has been attributed to negative hyperconjugation and inductive effects due to the presence of electron-withdrawing $-CF_3$ groups, meaning the additional electron density is localized on/near one of the highly electronegative F atoms. While we were unable to measure the VDE values for these larger molecules, the measurement of their EA $_0$ values adds to the current body of EA values for PFCs.

Overall, this study suggests that stable perfluorocarbons, including aromatic species, can be formed directly or in kinetically favorable secondary reactions during thermal decomposition of GF.

ASSOCIATED CONTENT

Supporting Information

The Supporting Information is available free of charge at https://pubs.acs.org/doi/10.1021/acs.jpcc.2c02180.

Table of chemical suppliers, GC data for species for which purity information was unavailable, a summary of laser shots associated with each PE spectrum, PE spectra of $C_6F_6^-$ and $^{GF}C_6F_6^-$ separated by polarization and shown on an expanded scale, raw PE spectra of all species, PE spectral fits for EA₀ approximation and VDE determination, binned and raw PE spectra from Figure 8 separated into both laser polarizations for all four species, superimposed PE spectra of $C_7F_{14}^-$ and CF_{3} - $C_6F_{11}^-$, side view of the anion and neutral structures of C_6F_6 , C_7F_8 , and C_5F_8 , and PE spectra of six species with

molecular structures showing trend in EA with size (PDF)

AUTHOR INFORMATION

Corresponding Author

Caroline Chick Jarrold — Department of Chemistry, Indiana University, Bloomington, Indiana 47405, United States; orcid.org/0000-0001-9725-4581; Email: cjarrold@indiana.edu

Authors

Brett A. Williams – Department of Chemistry, Indiana University, Bloomington, Indiana 47405, United States

A. R. Siedle – Department of Chemistry, Indiana University, Bloomington, Indiana 47405, United States; ocid.org/0000-0003-3591-5633

Complete contact information is available at: https://pubs.acs.org/10.1021/acs.jpcc.2c02180

Notes

The authors declare no competing financial interest.

ACKNOWLEDGMENTS

The authors are grateful for assistance with the computational portion of this study provided by Dr. Marissa Dobulis of the Indiana University Department of Chemistry. The authors also thank Angela Hansen of the Indiana University Department of Chemistry Mass Spectrometry Facility for her assistance with the GC-MS. The authors gratefully acknowledge support for this research from the National Science Foundation, Grant CHE-2053889.

REFERENCES

- (1) Kajdas, C.; Karpińska, A.; Kulczycki, A. Industrial Lubricants. In *Chemistry and Technology of Lubricants*; Mortier, R. M., Fox, M. F., Orszulik, S. T., Eds.; Springer Netherlands: Dordrecht, 2010; pp 239–292.
- (2) Noël, S.; Boyer, L.; Bodin, C. X-Ray Photoelectron Spectroscopy Investigation of Fluorocarbon Lubricant Films. *J. Vac. Sci. Technol. A* **1991**, *9*, 32–38.
- (3) Eastoe, J.; Bayazit, Z.; Martel, S.; Steytler, D. C.; Heenan, R. K. Droplet Structure in a Water-in-CO₂ Microemulsion. *Langmuir* **1996**, 12, 1423–1424.
- (4) Wang, S.; Marchant, R. E. Fluorocarbon Surfactant Polymers: Effect of Perfluorocarbon Branch Density on Surface Active Properties. *Macromolecules* **2004**, *37*, 3353–3359.
- (5) Wu, W.; Wang, J.; Zhou, Y.; Sun, Y.; Zhou, X.; Zhang, A. Design, Synthesis and Application of Short-Chained Perfluorinated Nitrogenous Heterocyclic Surfactants for Hydrocarbon Subphases. *J. Fluorine Chem.* **2021**, 252, 109919.
- (6) Barthel-Rosa, L. P.; Gladysz, J. A. Chemistry in Fluorous Media: A User's Guide to Practical Considerations in the Application of Fluorous Catalysts and Reagents. *Coord. Chem. Rev.* **1999**, *190*–*192*, 587–605.
- (7) Crampton, M. R.; Cropper, E. L.; Gibbons, L. M.; Millar, R. W. The Nitration of Arenes in Perfluorocarbon Solvents. *Green Chem.* **2002**, *4*, 275–278.
- (8) Miller, M. A.; Sletten, E. M. A General Approach to Biocompatible Branched Fluorous Tags for Increased Solubility in Perfluorocarbon Solvents. *Org. Lett.* **2018**, *20*, 6850–6854.
- (9) Bolaji, B. O.; Huan, Z. Performance Investigation of Some Hydro-Fluorocarbon Refrigerants with Low Global Warming as Substitutes to R134a in Refrigeration Systems. *J. Eng. Thermophys.* **2014**, 23, 148–157.

- (10) Sicard, A. J.; Baker, R. T. Fluorocarbon Refrigerants and Their Syntheses: Past to Present. *Chem. Rev.* **2020**, *120*, 9164–9303.
- (11) Von Der Hardt, K.; Schoof, E.; Kandler, M. A.; Dötsch, J.; Rascher, W. Aerosolized Perfluorocarbon Suppresses Early Pulmonary Inflammatory Response in a Surfactant-Depleted Piglet Model. *Pediatr. Res.* **2002**, *51*, 177–182.
- (12) Murgia, X.; Gastiasoro, E.; Mielgo, V.; Alvarez-Diaz, F.; Lafuente, H.; Valls-i-Soler, A.; Gomez-Solaetxe, M. A.; Larrabe, J. L.; Rey-Santano, C. Surfactant and Perfluorocarbon Aerosolization by Means of Inhalation Catheters for the Treatment of Respiratory Distress Syndrome: An *In Vitro* Study. *J. Aerosol Med. Pulm. D* 2011, 24, 81–87.
- (13) Bleyl, J. U.; Ragaller, M.; Tscho, U.; Regner, M.; Kanzow, M.; Hubler, M.; Rasche, S.; Albrecht, M. Vaporized Perfluorocarbon Improves Oxygenation and Pulmonary Function in an Ovine Model of Acute Respiratory Distress Syndrome. *Anesthesiology* **1999**, *91*, 461–469.
- (14) Cabrales, P.; Vazquez, B. Y. S.; Negrete, A. C.; Intaglietta, M. Perfluorocarbons as Gas Transporters for O₂, NO, CO and Volatile Anesthetics. *Transfus. Altern. Transfus. Med.* **2007**, *9*, 294–303.
- (15) Chen, H.-S.; Yang, Z.-H. Perfluorocarbon as Blood Substitute in Clinical Applications and in War Casualties. *Biomater. Artif. Cell.* **1988**, *16*, 403–409.
- (16) Keyhanian, S.; Ebrahimifard, M.; Zandi, M. Investigation on Artificial Blood or Substitute Blood Replace the Natural Blood. *Iran. J. Pediatr. Hematol. Oncol.* **2014**, *4*, 72–77.
- (17) Shaffer, T. H.; Wolfson, M. R.; Clark Jr, L. C. Liquid Ventilation. *Pediatr. Pulm.* **1992**, *14*, 102–109.
- (18) Fuhrman, B. P.; Hernan, L. J.; Holm, B. A.; Leach, C. L.; Papo, M. C.; Steinhorn, D. M. Perfluorocarbon Associated Gas Exchange (Page): Gas Ventilation of the Perfluorocarbon Filled Lung. *Artif. Cell. Blood Sub.* **1994**, *22*, 1133–1139.
- (19) Riess, J. G. Oxygen Carriers ("Blood Substitutes") Raison D'etre, Chemistry, and Some Physiology Blut Ist Ein Ganz Besondrer Saft. *Chem. Rev.* **2001**, *101*, 2797–2920.
- (20) Begley, P.; Foulger, B.; Simmonds, P. Femtogram Detection of Perfluorocarbon Tracers Using Capillary Gas Chromatography-Electron-Capture Negative Ion Chemical Ionisation Mass Spectrometry. *J. Chromatogr. A* **1988**, *445*, 119–128.
- (21) Watson, T. B.; Wilke, R.; Dietz, R. N.; Heiser, J.; Kalb, P. The Atmospheric Background of Perfluorocarbon Compounds Used as Tracers. *Environ. Sci. Technol.* **2007**, *41*, 6909–6913.
- (22) Matthews, J. C.; Bacak, A.; Khan, M. A. H.; Wright, M. D.; Priestley, M.; Martin, D.; Percival, C. J.; Shallcross, D. E. Urban Pollutant Transport and Infiltration into Buildings Using Perfluor-ocarbon Tracers. *Int. J. Env. Res. Pub. He.* **2017**, *14*, 214.
- (23) King, R. A.; Pettigrew, N. D.; Schaefer, H. F. The Electron Affinities of the Perfluorocarbons C_2F_n , n=1-6. *J. Chem. Phys.* **1997**, 107, 8536–8544.
- (24) Xie, Y.; Schaefer, H. F.; Cotton, F. A. The Radical Anions and the Electron Affinities of Perfluorinated Benzene, Naphthalene and Anthracene. *Chem. Commun.* **2003**, *39*, 102–103.
- (25) Bera, P. P.; Horný, L.; Schaefer, H. F. Cyclic Perfluorocarbon Radicals and Anions Having High Global Warming Potentials (GWPs): Structures, Electron Affinities, and Vibrational Frequencies. *J. Am. Chem. Soc.* **2004**, *126*, 6692–6702.
- (26) Paul, A.; Wannere, C. S.; Schaefer, H. F. Do Linear-Chain Perfluoroalkanes Bind an Electron? *J. Phys. Chem. A* **2004**, *108*, 9428–9434.
- (27) Li, Q.-s.; Feng, X.-j.; Xie, Y.; Schaefer, H. F. Electron Affinities of Perfluoro Polycyclic Aromatic Hydrocarbon Radicals: C_6F_5 , $C_{10}F_7$, and $C_{14}F_9$. *J. Phys. Chem. A* **2004**, *108*, 7071–7078.
- (28) Paul, A.; Wannere, C. S.; Kasalova, V.; Schleyer, P. v. R.; Schaefer, H. F. The Peculiar Trend of Cyclic Perfluoroalkane Electron Affinities with Increasing Ring Size. *J. Am. Chem. Soc.* **2005**, *127*, 15457–15469.
- (29) Feng, X.-j.; Li, Q.-s.; Xie, Y.; Schaefer, H. F. The Perfluoroadamantyl Radicals $C_{10}F_{15}$ and Their Anions. *J. Chem. Theory Comput.* **2005**, *1*, 279–285.

- (30) Li, Q.-s.; Feng, X.-j.; Xie, Y.; Schaefer, H. F. Perfluoroada-mantane and Its Negative Ion. J. Phys. Chem. A 2005, 109, 1454–1457.
- (31) Paul, A.; Schleyer, P. R.; Schaefer, H. F. High Electron Affinities of Bicyclo[n,n,0]perfluoroalkanes. *Mol. Phys.* **2006**, *104*, 1311–1324.
- (32) Feng, X.; Li, Q.; Gu, J.; Cotton, F. A.; Xie, Y.; Schaefer, H. F. Perfluorinated Polycyclic Aromatic Hydrocarbons: Anthracene, Phenanthrene, Pyrene, Tetracene, Chrysene, and Triphenylene. *J. Phys. Chem. A* **2009**, *113*, 887–894.
- (33) Zhang, X.; Li, Q.-S.; Xie, Y.; Schaefer, H. F. The Lowest Triplet Electronic States of Polyacenes and Perfluoropolyacenes. *Mol. Phys.* **2007**, *105*, 2743–2752.
- (34) Dimitrakopoulos, C. D.; Malenfant, P. R. L. Organic Thin Film Transistors for Large Area Electronics. *Adv. Mater.* **2002**, *14*, 99–117.
- (35) Mattheus, C. C.; de Wijs, G. A.; de Groot, R. A.; Palstra, T. T. M. Modeling the Polymorphism of Pentacene. *J. Am. Chem. Soc.* **2003**, 125, 6323–6330.
- (36) Kivelson, S.; Chapman, O. L. Polyacene and a New Class of Quasi-One-Dimensional Conductors. *Phys. Rev. B* **1983**, 28, 7236–7243.
- (37) Eustis, S. N.; Wang, D.; Bowen, K. H.; Patwari, G. N. Photoelectron Spectroscopy of Hydrated Hexafluorobenzene Anions. *J. Chem. Phys.* **2007**, *127*, 114312.
- (38) Rogers, J. P.; Anstöter, C. S.; Bull, J. N.; Curchod, B. F. E.; Verlet, J. R. R. Photoelectron Spectroscopy of the Hexafluorobenzene Cluster Anions: $(C_6F_6)_n^-$ (n = 1–5) and I- (C_6F_6) . *J. Phys. Chem. A* **2019**, 123, 1602–1612.
- (39) Nakajima, A.; Taguwa, T.; Hoshino, K.; Sugioka, T.; Naganuma, T.; Oho, F.; Watanabe, K.; Nakao, K.; Konishi, Y.; Kishi, R.; Kaya, K.; et al. Photoelectron Spectroscopy of $(C_6F_6)_n^-$ and $(Au-C_6F_6)^-$ Clusters. *Chem. Phys. Lett.* **1993**, 214, 22–26.
- (40) Fusaro, R. L.; Sliney, H. E. Graphite Fluoride (CF_x)_n—a New Solid Lubricant. *ASLE Trans.* **1970**, *13*, 56–65.
- (41) Ye, X.; Ma, L.; Yang, Z.; Wang, J.; Wang, H.; Yang, S. Covalent Functionalization of Fluorinated Graphene and Subsequent Application as Water-Based Lubricant Additive. *ACS Appl. Mater. Interfaces* **2016**, *8*, 7483–7488.
- (42) Ishida, Y.; Kusuno, H.; Watanabe, N. Dry Film Lubricant Consisting of Synthetic Resin, Fluorinated Graphite, and Solid Lubricants Such as Molybdenum Disulfide, Graphite, and Polytetra-fluoroethylene. US 3776845 A, 1973.
- (43) Watanabe, N. Characteristics and Applications of Graphite Fluoride. *Physica B+C* **1981**, *105*, 17–21.
- (44) Sun, C.; Feng, Y.; Li, Y.; Qin, C.; Zhang, Q.; Feng, W. Solvothermally Exfoliated Fluorographene for High-Performance Lithium Primary Batteries. *Nanoscale* **2014**, *6*, 2634–2641.
- (45) Ho, K.-I.; Huang, C.-H.; Liao, J.-H.; Zhang, W.; Li, L.-J.; Lai, C.-S.; Su, C.-Y. Fluorinated Graphene as High Performance Dielectric Materials and the Applications for Graphene Nanoelectronics. *Sci. Rep.* **2015**, *4*, 5893.
- (46) Jeon, K.-J.; Lee, Z.; Pollak, E.; Moreschini, L.; Bostwick, A.; Park, C.-M.; Mendelsberg, R.; Radmilovic, V.; Kostecki, R.; Richardson, T. J.; et al. Fluorographene: A Wide Bandgap Semiconductor with Ultraviolet Luminescence. ACS Nano 2011, 5, 1042–1046.
- (47) Hany, P.; Yazami, R.; Hamwi, A. Low-Temperature Carbon Fluoride for High Power Density Lithium Primary Batteries. *J. Power Sources* **1997**, *68*, 708–710.
- (48) Nakajima, T.; Gupta, V.; Ohzawa, Y.; Iwata, H.; Tressaud, A.; Durand, E. Electrochemical Properties and Structures of Surface-Fluorinated Graphite for the Lithium Ion Secondary Battery. *J. Fluorine Chem.* **2002**, *114*, 209–214.
- (49) Miao, X.; Yang, J.; Pan, W.; Yuan, H.; Nuli, Y.; Hirano, S.-i. Graphite Fluoride as a Cathode Material for Primary Magnesium Batteries with High Energy Density. *Electrochim. Acta* **2016**, 210, 704–711.
- (50) Kuriakose, A. K.; Margrave, J. L. Mass Spectrometric Studies of the Thermal Decomposition of Poly(Carbon Monofluoride). *Inorg. Chem.* **1965**, *4*, 1639–1641.

- (51) Kamarchik, P.; Margrave, J. L. Poly(Carbon Monofluoride): A Solid, Layered Fluorocarbon. Acc. Chem. Res. 1978, 11, 296–300.
- (52) Kamarchik, P.; Margrave, J. L. A Study of Thermal Decomposition of the Solid-Layered Fluorocarbon, Poly(Carbon Monofluoride). *J. Therm. Anal.* **1977**, *11*, 259–270.
- (53) Watanabe, N.; Koyama, S.; Imoto, H. Thermal Decomposition of Graphite Fluoride. I. Decomposition Products of Graphite Fluoride, (CF)_n in a Vacuum. *Bull. Chem. Soc. Jpn.* **1980**, 53, 2731–2734.
- (54) Williams, B. A.; Siedle, A. R.; Jarrold, C. C. Evidence of CF_2 Loss from Fluorine-Rich Cluster Anions Generated from Laser Ablation of Graphite Fluoride. *J. Phys. Chem. A* **2018**, 122, 9894–9900
- (55) Moravec, V. D.; Jarrold, C. C. Study of the Low-Lying States of NiO⁻ and NiO Using Anion Photoelectron Spectroscopy. *J. Chem. Phys.* **1998**, *108*, 1804–1810.
- (56) Dietz, T. G.; Duncan, M. A.; Powers, D. E.; Smalley, R. E. Laser Production of Supersonic Metal Cluster Beams. *J. Chem. Phys.* **1981**, 74. 6511–6512.
- (57) Waller, S. E.; Mann, J. E.; Jarrold, C. C. Asymmetric Partitioning of Metals among Cluster Anions and Cations Generated Via Laser Ablation of Mixed Aluminum/Group 6 Transition Metal Targets. J. Phys. Chem. A 2013, 117, 1765–1772.
- (58) Weyssenhoff, H. v.; Selzle, H. L.; Schlag, E. W. Laser-Desorbed Large Molecules in a Supersonic Jet. Z. Naturforsch. A 1985, 40, 674–676.
- (59) Stokes, S. T.; Li, X.; Grubisic, A.; Ko, Y. J.; Bowen, K. H. Intrinsic Electrophilic Properties of Nucleosides: Photoelectron Spectroscopy of Their Parent Anions. *J. Chem. Phys.* **2007**, *127*, 084321.
- (60) Boesl, U.; Bäßmann, C.; Drechsler, G.; Distelrath, V. Laser-Based Ion Source for Mass Spectrometry and Laser Spectroscopy of Negative Ions. *Eur. J. Mass Spectrom.* **1999**, *5*, 455–470.
- (61) Chalamala, B. R.; Pack, S. P.; Rowell, C. A. Field Emission Device. US 6091190 A, July 18, 2000.
- (62) Fomenko, V. S. Handbook of Thermionic Properties, 1st ed.; Plenum Press: New York, 1966.
- (63) Akin, F. A.; Jarrold, C. C. Separating Contributions from Multiple Structural Isomers in Anion Photoelectron Spectra: Al₃O₃⁻ Beam Hole Burning. *J. Chem. Phys.* **2003**, *118*, 1773–1778.
- (64) Frisch, M. J.; Trucks, G. W.; Schlegel, H. B.; Scuseria, G. E.; Robb, M. A.; Cheeseman, J. R.; Scalmani, G.; Barone, V.; Petersson, G. A.; Nakatsuji, H.; et al. *Gaussian 16, Rev. C.01*; Wallingford, CT, 2016.
- (65) Hiraoka, K.; Fujita, K.; Ishida, M.; Ichikawa, T.; Okada, H.; Hiizumi, K.; Wada, A.; Takao, K.; Yamabe, S.; Tsuchida, N. Gas-Phase Ion/Molecule Reactions in C_5F_8 . *J. Phys. Chem. A* **2005**, *109*, 1049–1056.
- (66) Miller, T. M.; Friedman, J. F.; Shuman, N. S.; Ard, S. G.; Melko, J. J.; Viggiano, A. A. Electron Attachment to C_7F_{14} , Thermal Detachment from $C_7F_{14}^-$, the Electron Affinity of C_7F_{14} , and Neutralization of $C_7F_{14}^-$ by Ar⁺. J. Phys. Chem. A **2012**, 116, 10293–10300.
- (67) Hou, X.-J.; Huang, M.-B. Structure of the Hexafluorobenzene Anion. J. Mol. Struct. Theochem 2003, 638, 209–214.
- (68) Wentworth, W. E.; Limero, T.; Chen, E. C. M. Electron Affinities of Hexafluorobenzene and Pentafluorobenzene. *J. Phys. Chem.* **1987**, 91, 241–245.
- (69) Dillow, G. W.; Kebarle, P. Substituent Effects on the Electron Affinities of Perfluorobenzenes C₆F₅X. *J. Am. Chem. Soc.* **1989**, 111, 5592–5596.
- (70) Chowdhury, S.; Grimsrud, E. P.; Heinis, T.; Kebarle, P. Electron Affinities of Perfluorobenzene and Perfluorophenyl Compounds. J. Am. Chem. Soc. 1986, 108, 3630–3635.
- (71) Lifshitz, C.; Tiernan, T. O.; Hughes, B. M. Electron Affinities from Endothermic Negative-Ion Charge-Transfer Reactions. IV. SF₆, Selected Fluorocarbons and Other Polyatomic Molecules. *J. Chem. Phys.* **1973**, *59*, 3182–3192.

- (72) Limão-Vieira, P.; Duflot, D.; Giuliani, A.; Vasekova, E.; Lourenço, J. M. C.; Santos, P. M.; Hoffmann, S. V.; Mason, N. J.; Delwiche, J.; Hubin-Franskin, M. J. Electronic State Spectroscopy of *c*-C₅F₈ Explored by Photoabsorption, Electron Impact, Photoelectron Spectroscopies and Ab Initio Calculations. *J. Phys. Chem. A* **2008**, *112*, 2782–2793.
- (73) Hayashi, T.; Ishikawa, K.; Sekine, M.; Hori, M. Dissociations of C_5F_8 and C_5HF_7 in Etching Plasma. *Jpn. J. Appl. Phys.* **2013**, *52*, 05FB02
- (74) Feil, S.; Märk, T. D.; Mauracher, A.; Scheier, P.; Mayhew, C. A. Investigations of Electron Attachment to the Perfluorocarbon Molecules c-C₄F₈, 2-C₄F₈, 1,3 C₄F₆, and c-C₅F₈. Int. J. Mass Spectrom. **2008**, 277, 41–51.
- (75) Wigner, E. P. On the Behavior of Cross Sections near Thresholds. *Phys. Rev.* **1948**, 73, 1002–1009.
- (76) Cooper, J.; Zare, R. N. Angular Distribution of Photoelectrons. *J. Chem. Phys.* **1968**, *48*, 942–943.
- (77) Sanov, A. Laboratory-Frame Photoelectron Angular Distributions in Anion Photodetachment: Insight into Electronic Structure and Intermolecular Interactions. *Annu. Rev. Phys. Chem.* **2014**, *65*, 341–363.
- (78) Jeong, S.-Y.; Shin, C.-H.; Kim, S.-J. Theoretical study on the structures and the electron affinities of cyclic perfluoroalkanes (c-PFA). *Anal. Sci. Technol.* **2013**, *26*, 51–60.
- (79) Mock, R. S.; Grimsrud, E. P. Electron Photodetachment of the Molecular Anions of SF₆ and Several Perfluorinated Hydrocarbons. *Chem. Phys. Lett.* **1991**, *184*, 99–101.
- (80) Chen, E. S.; Chen, E. C. M.; Barrera, L. K.; Herder, C. Atmospheric Pressure Anion Mass Spectrometry: Electron Affinities and Activation Energies of Thermal Electron Attachment Perfluoromethylcyclohexane, C₇F₁₄. Rapid Commun. Mass Spectrom. **2015**, 29, 1165–1177.
- (81) Grimsrud, E. P.; Chowdhury, S.; Kebarle, P. Electron Affinity of SF_6 and Perfluoromethylcyclohexane. The Unusual Kinetics of Electron Transfer Reactions $A^-+B=A+B^-$, Where $A=SF_6$ or Perfluorinated Cyclo-Alkanes. *J. Chem. Phys.* **1985**, *83*, 1059–1068.

□ Recommended by ACS

The Thermal Dissociation–Recombination Reactions of SiF_4 , SiF_3 , and SiF_2 : A Shock Wave and Theoretical Modeling Study

Carlos J. Cobos, Jürgen Troe, et al.

NOVEMBER 18, 2022

THE JOURNAL OF PHYSICAL CHEMISTRY A

READ 🖸

Reaction of Cl Atom with c-C₅F₈ and c-C₅HF₇: Relative and Absolute Measurements of Rate Coefficients and Identification of Degradation Products

Tomasz Gierczak, James B. Burkholder, et al.

OCTOBER 15, 2022

THE JOURNAL OF PHYSICAL CHEMISTRY A

READ 🗹

Electron Driven Reactions in Tetrafluoroethane: Positive and Negative Ion Formation

João Pereira-da-Silva, Filipe Ferreira da Silva, et al.

MAY 17, 2021

JOURNAL OF THE AMERICAN SOCIETY FOR MASS SPECTROMETRY

READ 🗹

Anionic Dimers of Fluorinated Alcohols

Konrad Koszinowski and Rene Rahrt

MAY 24, 2022

JOURNAL OF THE AMERICAN SOCIETY FOR MASS SPECTROMETRY

READ 🗹

Get More Suggestions >